Chapter 3

Identification of Coumarin-Based Natural Compounds as Potential VEGFR-2 Inhibitors

3 Identification of Coumarin-based Natural Compounds as Potential VEGFR-2 Inhibitors

3.1 Introduction

Coumarins are secondary metabolites obtained extensively from plants and also from microorganisms and fungi [79]. The molecule gets its name from '*coumarou*,' a French word for Tonka beans (seeds of *Dipteryx odorata*) from which they were first [80]. More than 1300 different coumarins have been reported from more than 150 plant species belonging principally to Apiaceae, Fabaceae, Asteraceae, Rutaceae, Moraceae, Oleaceae, and Thymelaeaceae families [80, 81]. Coumarin is a versatile nucleus with different substitution sites and potent pharmacophore contributing to its broad pharmacological spectrum. Coumarins possess antioxidant (osthole), anticancer (xanthotoxol), antibacterial (agasyllin), antitubercular (bergapten), antiviral (calanolide A), anti-inflammatory (imperatorin), neuroprotective (esculetin), anticoagulant (dicumarol), antidiabetic (fraxidin), and photosensitizing (methoxsalen) activities [79, 81]. Amidst coumarin's broad spectrum of pharmacology, its anticancer potential is quite fascinating as many natural coumarins possess anticancer activity- esculetin, osthole, chartreusin, fraxin, imperatorin, umbelliferone, daphnetin, auroptene, psoralen, oxypeucedanin, seselin, etc. [81, 82]. Various synthetic derivatives of coumarins are reported to exhibit potent antitumor and anticancer potential [83-85]. Coumarins act as anticancer agents via different mechanisms- inhibition of mitosis, cell-cycle arrest, angiogenesis, inhibition of telomerase, hsp90, etc. [82, 86]. Amongst various anticancer mechanisms of coumarins, only a few studies have been done on their anti-angiogenic activity [87, 88].

Vascular endothelial growth factor receptors (VEGFRs) are a type of receptor tyrosine kinases involved in angiogenesis and bind to vascular endothelial growth factors (VEGFs) to produce their angiogenic effect and aid tumor growth and survival [89, 90].

There are three types of VEGFRs- 1, 2, and 3, and among them, VEGFR-2 is expressed on most epithelial cells and principally involved in angiogenesis during cancer [91]. The human VEGFR-2 receptor is a 1356 amino acid protein containing kinase insert domain (KDR) [92]. VEGFR-2 signaling pathway involves its binding with VEGF-A, resulting in VEGFR-2 dimerization and activation of downstream signaling pathways such as PLCγ-PKC-MEK-ERK pathway, TSAd-Src-PI3K-Akt pathway, PLCγ-PKC-eNOS-NO and TSAd-Src-PI3K-Akt pathway; SHB-PI3K-Rac, SHB-FAK-paxillin, and NCK-p38-MAPKAPK2/3 pathway [92, 93].

Angiogenesis is the primary requisite of tumors for their sustenance, growth, proliferation, and survival; hence, they interfere with the body's homeostasis and increase the secretion of angiogenic factors. This results in overexpression and increased kinase activity of VEGFR-2 due to increased VEGF secretion [94]. Thus, the inhibition of VEGFR-2 is considered an attractive approach to target tumor-related angiogenesis and subsequent tumor growth [95]. Several FDA-approved VEGFR-2 inhibitors- sorafenib, lenvatinib, sunitinib, vandetanib, and axitinib- are already used for different types of cancers. These inhibitors exert their action by blocking the VEGF-mediated activation of VEGFR-2 receptors and their subsequent signaling [96].

In this work, a pharmacophore-based virtual screening to identify the potential coumarin leads from the COCONUT database of NPs against VEGFR-2 was conducted. The literature search showed that no high-throughput virtual screening (HTVS) studies are performed on a natural coumarin database against VEGFR-2 protein. So, we tried to identify natural coumarins as potential VEGFR-2 inhibitors by rigorous *in silico* studies. The approach encompassed several key methodologies- feature-based pharmacophore screening of the coumarin database, high-throughput docking studies, and molecular dynamic (MD) studies on the identified hits for determining potent angiogenic inhibitors.

3.2 Experimental section

3.2.1 Database

The COCONUT database was used for performing pharmacophore-based virtual screening [97]. The database consisted of 407270 entries of NPs and was processed in the KNIME analytics platform (https://www.knime.com/) to obtain molecules with only a 'coumarin' scaffold [98]. The 'substructure search' node was used to accomplish this, where the coumarin scaffold was drawn and executed. Later, the duplicate ligands were filtered out using the 'duplicate row filter' node. This resulted in 20614 molecules with coumarin scaffold that were used for further studies.

3.2.2 e-pharmacophore generation and pharmacophore-based virtual screening

The crystallographic structure of VEGFR-2 protein complexed with multikinase inhibitor lenvatinib (PDB: 3WZD) was obtained from the protein data bank in PDB format [99] (https://www.rcsb.org/). The PDB 3WZD was selected as it was the only entry in protein data bank where lenvatinib was complexed with VEGFR-2. The chosen PDB had a resolution of 1.57 Å and R-value work of 0.181. The structure of VEGFR-2 with co-crystallized ligand and active site is represented in Figure 3.1. The interaction of lenvatinib with VEGFR-2 was studied on Discovery Studio 2021[100]. The pharmacophoric features of lenvatinib interacting with receptors such as hydrophobic, hydrogen-bond acceptor, hydrogen-bond donor, and aromatic ring were chosen for pharmacophore model generation. The pharmacophore-based virtual screening of coumarins using pharmacophoric features of lenvatinib was performed using the Pharmit server (https://pharmit.csb.pitt.edu/) [101]. In the server, the pharmacophoric search was limited to 'one conformer per molecule' and 'one molecule per hit.'

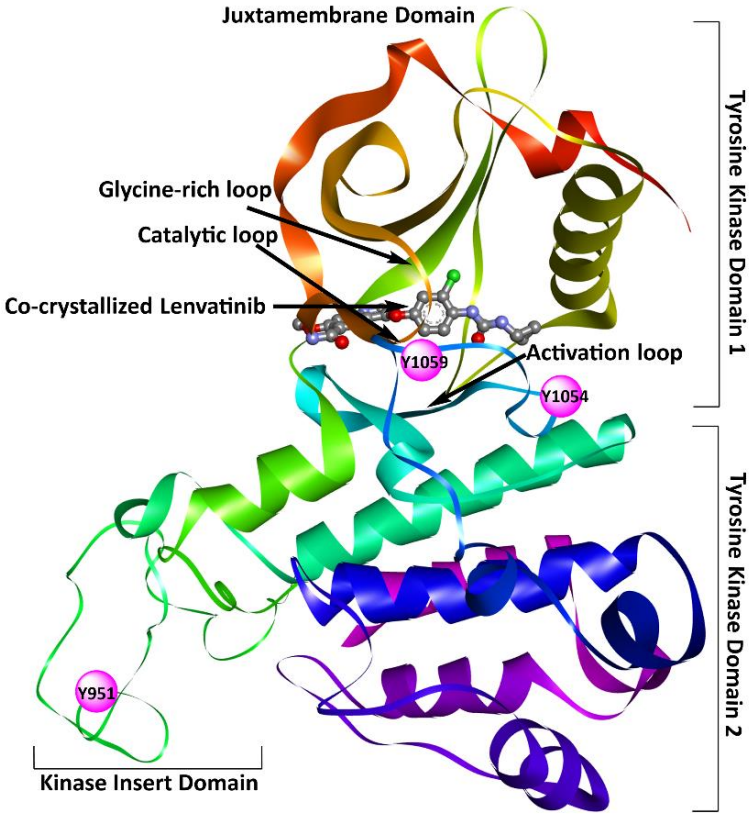

Figure 3.1 Crystal structure of VEGFR-2 protein (PDB: 3WZD) in complex with lenvatinib.

3.2.3 Homology modeling & model validation

Homology modeling is a highly accurate and successful method for predicting the tertiary structure of query protein using template protein and sequence alignment [102]. It is based on the assumption that proteins share structural similarity owing to common evolutionary ancestry, and based on this concept the 3D structure of the target protein could be determined using known homologous protein as a template [103]. The VEGFR-2 protein structure was viewed in UCSF Chimera 1.14 to check missing residues [104]. The missing residues in the protein were filled using homology modeling performed via SwissModel (https://swissmodel.expasy.org/) using the user template interface [105]. The FASTA sequence of the protein was obtained from a protein data bank, and the PDB: 3WZD was used as a PDB template to build the homology model.

The quality of the original protein and modelled protein was evaluated and compared to check the accuracy of the homology build protein. The SwissModel server provides QMEAN and the Global Model Quality Estimate (GMQE) parameters to assess the quality. Other web tools, viz. Molprobity (http://molprobity.biochem.duke.edu) and SAVESv6.0 (https://saves.mbi.ucla.edu/) were also used. The protein validation parameters of Molprobity are protein geometry (Ramachandran plot, Cβ deviation, rotamers, MolProbity score) and all-atom contacts (Clashscore). The SAVESv6.0 is a protein structure validation server consisting of different protein validation programs, viz. ERRAT, VERIFY 3D, and PROCHECK. ERRAT evaluates improvement and refinement in the modelled protein structure [102]. PROCHECK evaluates the quality of modelled protein by Ramachandran plot, bond angle, torsion angles, atomic distances, and surface area [102].

3.2.4 Energy minimization and preparation of protein

PDB2PQR server was used to assign the correct protonation state to the protein residues at pH 7.4 (https://server.poissonboltzmann.org/pdb2pqr) [106]. The energy minimization of the modelled VEGFR-2 protein was performed using Pmemd module of Amber 20. The energy minimization parameters were 1000 steps of conjugate gradient, 4000 steps of steepest descent, and 0.02 Å step size. After energy minimization, the protein was processed in AutoDockTools-1.5.7 by adding polar hydrogens only, merging non-polar hydrogens, adding Gastieger charge, and finally converted into PDBQT format [107].

3.2.5 Ligand preparation

The ligands obtained after pharmacophore-based virtual screening and PAINS filtering were processed before docking studies. The first step included ligand energy minimization to remove stearic clashes in the ligand and bring them to energetically favourable spatial conformation. The ligand energy minimization was performed on Open

Bable 3.1.1 software that uses Generalized Amber Force Field with 4000 steps of steepest descent algorithm [108]. Finally, the minimized ligands were converted to AutoDock compatible PDBQT format using MGL tools 1.5.7 rc [109].

3.2.6 Grid generation and validation

The interaction of lenvatinib and VEGFR-2 was visualized using Discovery Studio 2021. The interacting residues were used as reference points for building a grid box around the active site [110]. The grid maps were calculated using Autogrid 4.0 [109]. The grid size of the minimized protein was set at XYZ points 48 X 62 X 76 with a grid spacing of 0.375 Å, and the grid centre was set at x, y, and z coordinates 1.311, –6.175, and 15.419, respectively. The grid validation was done by redocking lenvatinib with VEGFR-2. The root-mean square deviation (RMSD) between heavy atoms of the co-crystallized lenvatinib and redocked lenvatinib was calculated using the Desmond Maestro package (D.E. Shaw Research, New York, USA).

3.2.7 HTVS and molecular docking study

HTVS is extensively used for screening big libraries of compounds to determine the binding affinity of the compounds with target receptor and uses a scoring function to do so [111]. The docking study was performed using AutoDock 4.2.6 and Lamarckian genetic algorithm (LGA) in three steps: 1) HTVS, 2) Standard precision (SP) docking, and 3) Extra precision (XP) docking. The coumarins were docked against VEGFR-2, and in each proceeding step, the docking protocol was made stringent to reduce the probability of false positives. The visualization and analysis of docking was performed using Discovery Studio 2021 [100].

3.2.8 *In silico* ADMET prediction

The *in silico* ADMET prediction of final hits was done using freely accessible web tool PreADMET (https://preadmet.webservice.bmdrc.org/) and SwissADME [112, 113]. The

parameters such as BBB penetration, buffer solubility, human intestinal absorption (HIA), hERG inhibition, carcinogenicity, and CYP2D6 inhibition were predicted.

3.2.9 MD simulation study

MD simulation is an important part of drug discovery as it provides insights into the motion of protein at different time intervals which could not be provided by NMR, XRD, etc [114]. When a drug binds to the active site of target protein it gives rise to conformational changes in protein structure that interferes with its normal function. Hence, to simulate the body's environment at the initial developmental stage, MD simulation studies are performed [115].

The MD studies of final hits with binding energy less than lenvatinib and cluster size more than lenvatinib were performed via Amber 20. The ligand-protein complex was obtained from Discovery Studio 2021 [100]. The complex's parameter and coordinate files were created using tleap and the Amber ff14SB force field. Utilizing TIP3P water molecules in a cubic periodic box with a 10 Å edge length, the refined structures were solvated. Sodium ions were added to the system to balance out its overall charge. Long-range electrostatic interactions were handled using the Particle Mesh Ewald (PME) approach and a non-bonded cut-off of 10 Å [110]. To refine the system, energy minimization was performed using a combination of steepest descent and conjugate gradient algorithms. The system was heated to 310 K using a Langevin thermostat and the collision frequency was tuned to 5 ps^{-1} using the NVT ensemble. Once the desired temperature was reached, a 100 ps MD run was carried out in the NPT ensemble at a pressure of 1 bar, using the Berendsen barostat. Subsequently, a 100 ns production MD simulation was performed once the system reached equilibrium. Using the *cpptraj* tool of Amber 20, the trajectories acquired from the MD simulations were examined for RMSD, root-mean-square fluctuation (RMSF), and radius of gyration (Rg) studies [107].

3.2.10 Binding free energy calculation

The calculation of binding free energy was executed via MMPBSA.py package of Amber 20 and comprised of molecular mechanics, Poisson-Boltzmann surface area (MM-PBSA) and molecular mechanics, Generalised Born model for solvent accessibility (MM-GBSA). The energy calculation was done using GB method in the last 50 ns of MD simulation at 10 ns interval. The salt concentration, inner dielectric, and exterior dielectric were set at 0.1 nM, 1, and 80, respectively.

3.3 Result & Discussion

3.3.1 e-pharmacophore generation and pharmacophore-based virtual screening

Lenvatinib is a small molecule multiple kinase inhibitor with IC_{50} value range between 4-100 nM. Figure 3.2 shows the pharmacophoric features of lenvatinib used for generating e-pharmacophore. The pharmacophore-based virtual screening of the COCONUT database using this e-pharmacophore resulted in 6301 hits. The RMSD cutoff was set at 0.5 Å and the molecules with RMSD less than that were selected for HTVS. This resulted in the final 910 hits. The molecular property distribution of the resulting hits are provided in Appendix (Figure A.1).

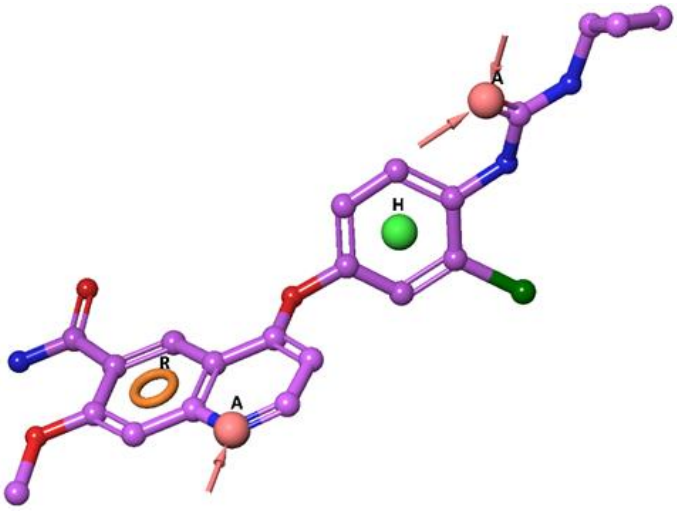

Figure 3.2 Pharmacophoric features of lenvatinib selected for virtual screening (A represents Hydrogen bond acceptor, H represents Hydrophobic, R represents Aromatic Ring).

3.3.2 Homology modeling and model validation

The structure alignment between the template and modelled protein was checked by superimposing them using 'Protein Structure Alignment' in Desmond Maestro. The alignment score and RMSD of the modelled VEGFR-2 protein were found to be 0.007 and 0.414 Å, respectively. The sequence alignment of template and modelled proteins is in Appendix (Figure A.2). The QMEAN Z-score was 0.89 ± 0.05 and validation results are provided in Appendix (Figure A.3).

The Ramachandran plot obtained from the Molprobity server showed 99.7 % residues in the allowed region and only 0.3% in the disallowed region with only one outlier residue, i.e., Asp 260. The Ramachandran plot obtained from PROCHECK indicated no residues in the disallowed region (Figure 3.3).

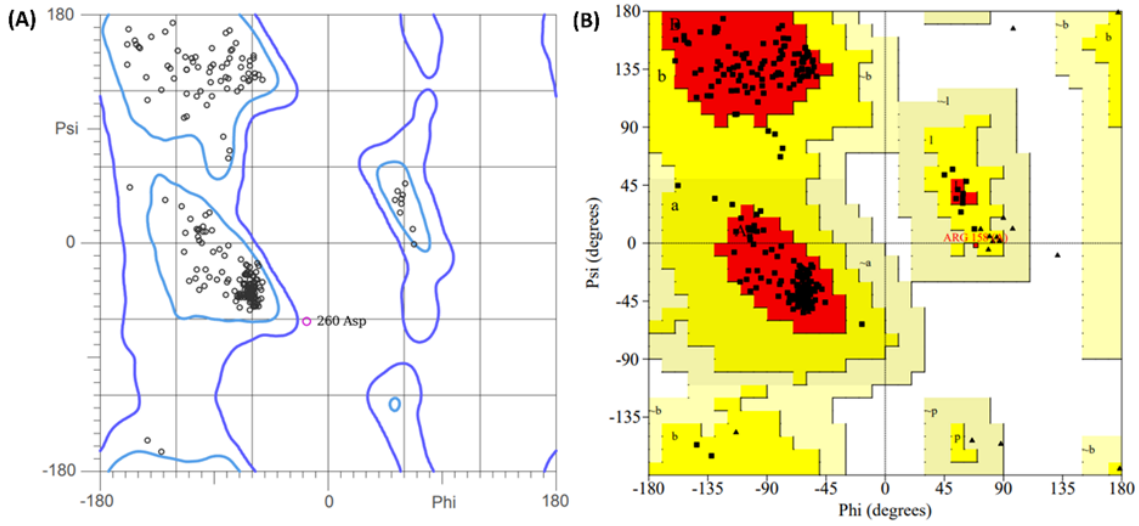

Figure 3.3 Ramachandran plot of homology model of VEGFR-2 protein obtained from- (A) Molprobity and (B) PROCHECK.

The Rama Z-score is a global metric for assessing the overall quality of homology-built model and a score between -2 to 2 is indicative of the normal backbone geometry of the model. The modelled protein had a Rama Z-score value of 1.49 ± 0.49, which was within permissible limits [116]. The Cβ deviation is the difference between the predicted position of the Cβ atom and its ideal expected position. The Cβ deviation greater than

0.25 Å indicates incompatibility in sidechain and mainchain conformation. No Cβ deviation (>0.25 Å) was found in the modeled protein [117]. The Clashscore is number of serious stearic clashes (>0.4 Å) per 1000 atoms including hydrogen atoms and for modeled protein it was 1.03 which is considered very good. MolProbity score is the weighted sum of clashes, Ramachandran favoured, and rotamer outliers and for modelled protein it was 0.80 [118].

ERRAT assesses the statistical properties of non-bonded interactions among various atom types within a model protein, comparing them to a database of dependable high-resolution structures [119]. The overall quality factor of the modelled protein on the ERRAT program was found to be 98.639 and the plot is shown in Appendix (Figure A.4). The VERIFY3D assesses how well a 3D atomic model aligns with its corresponding 1D amino acid sequence [120]. In this, at least 80% amino acids of the modelled protein should score >=0.1 in 3D/1D profile for model to be considered good. In the modelled VEGFR-2 protein, 85.48% of the residues were found to have average 3D/1D score >=0.1 and the plot is shown in Appendix (Figure A.4).

3.3.3 Energy minimization and preparation of protein

The potential energy of the system was minimized from -276910 kcal/mol to -420330 kcal/mol and the graph depicting the same is provided in the Appendix (Figure A.5).

3.3.4 Grid generation and validation

Lenvatinib displayed hydrophobic and hydrogen bond interactions with the active site residues of VEGFR-2, viz. Glu 885, Ile 888, Leu 889, Cys 919, Cys 1045, Asp 1046, Phe 1047. The RMSD between the two pose was found to be 0.9280 Å and the poses are shown in the Appendix (Figure A.6).

3.3.5 HTVS and molecular docking study

Coumarins from the COCONUT database were docked against the VEGFR-2 receptor protein (PDB Id: 3WZD). Lenvatinib was employed as an internal reference for selecting the compounds. In HTVS, the ligands having binding energy less than lenvatinib were filtered out for further SP docking. The HTVS was performed on a total 909 ligands and from that, 485 compounds were selected for SP docking. From SP docking, 30 compounds were chosen for XP docking as their binding energy was less than reference. Through XP docking, the compounds were tapered to 12 and the docking was analyzed and visualized using Discovery Studio [100]. Among 12 compounds, three compounds viz. CNP0056360, CNP0340213, and CNP036628 (Figure 3.4) with good binding energy, cluster size (Table 3.1) and ADMET properties were selected for further MD studies. The energy minimization, temperature, and density plots of selected ligands and lenvatinib is provided in Appendix (Figure A.7-A.10). The interaction diagrams of CNP0056360, CNP0340213, and CNP036628 with VEGFR-2 protein along with lenvatinib are shown in Figure 3.5. The binding energy, ligand efficiency, and cluster size of the rest of the compounds is provided in Appendix (Table A.1).

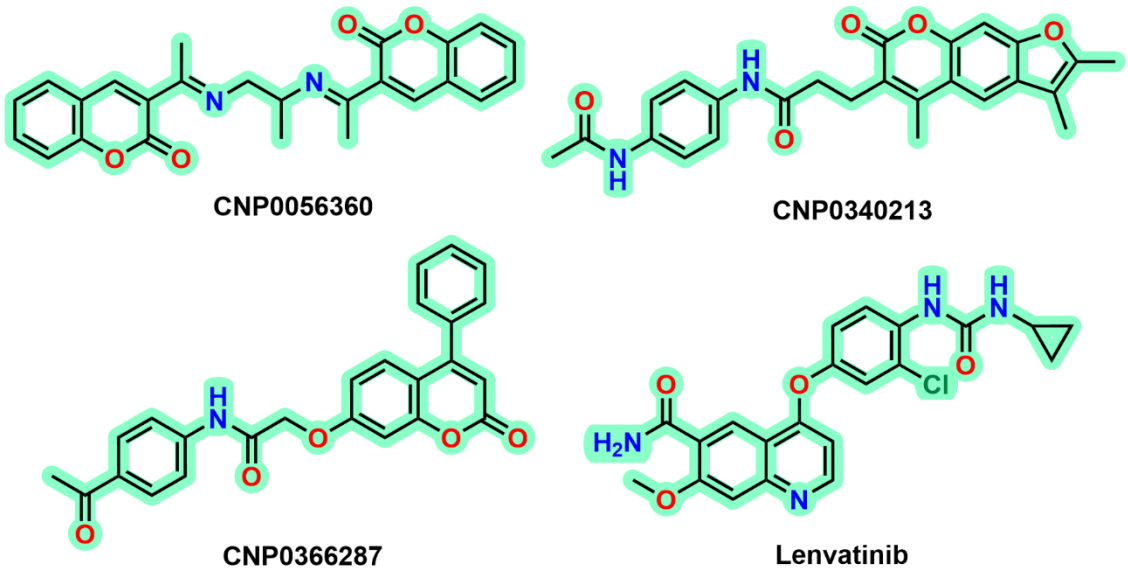

Figure 3.4 Structures of final hits and standard.

Table 3.1 Summary of interactions of final hits and lenvatinib with VEGFR-2 protein.

COCONUT database ID	**Binding Energy (kcal/mol)**	**Ligand Efficiency (kcal/mol)**	**Cluster size**	**Total poses**	**Interactions with VEGFR-2 (PDB:3WZD)**
CNP0056360	-13.41	-0.433	43	100	A:Leu 840 (Pi-Sigma), A:Cys 919 (H-Bond), A:Cys 1045 (Pi-Sulfur), A:Asp 1046 (H-Bond), A:Phe 1047 (Pi-Pi T-shaped)
CNP0340213	-12.91	-0.403	45	100	A:Glu 885 (Pi-Anion), A:Phe 918 (Pi-Pi Stacked), A:Cys 919 (H-Bond), A:Asp 1046 (H-Bond), A:Phe 1047 (Pi-Sigma)
CNP0366287	-12.68	-0.409	39	100	A:Lys 868 (H-Bond), A:Cys 919 (H-Bond), A:Asn 923 (H-Bond) A:Asp 1046 (Pi-Anion), A:Phe 1047 (Pi-Pi T-shaped)
Lenvatinib	-11.37	-0.379	32	100	A:Leu 840 (Pi-Sigma), A:Glu 885 (H-Bond), A:Cys 919 (H-Bond), A:Cys 1045 (Pi-Sulfur), A:Asp 1046 (H-Bond)

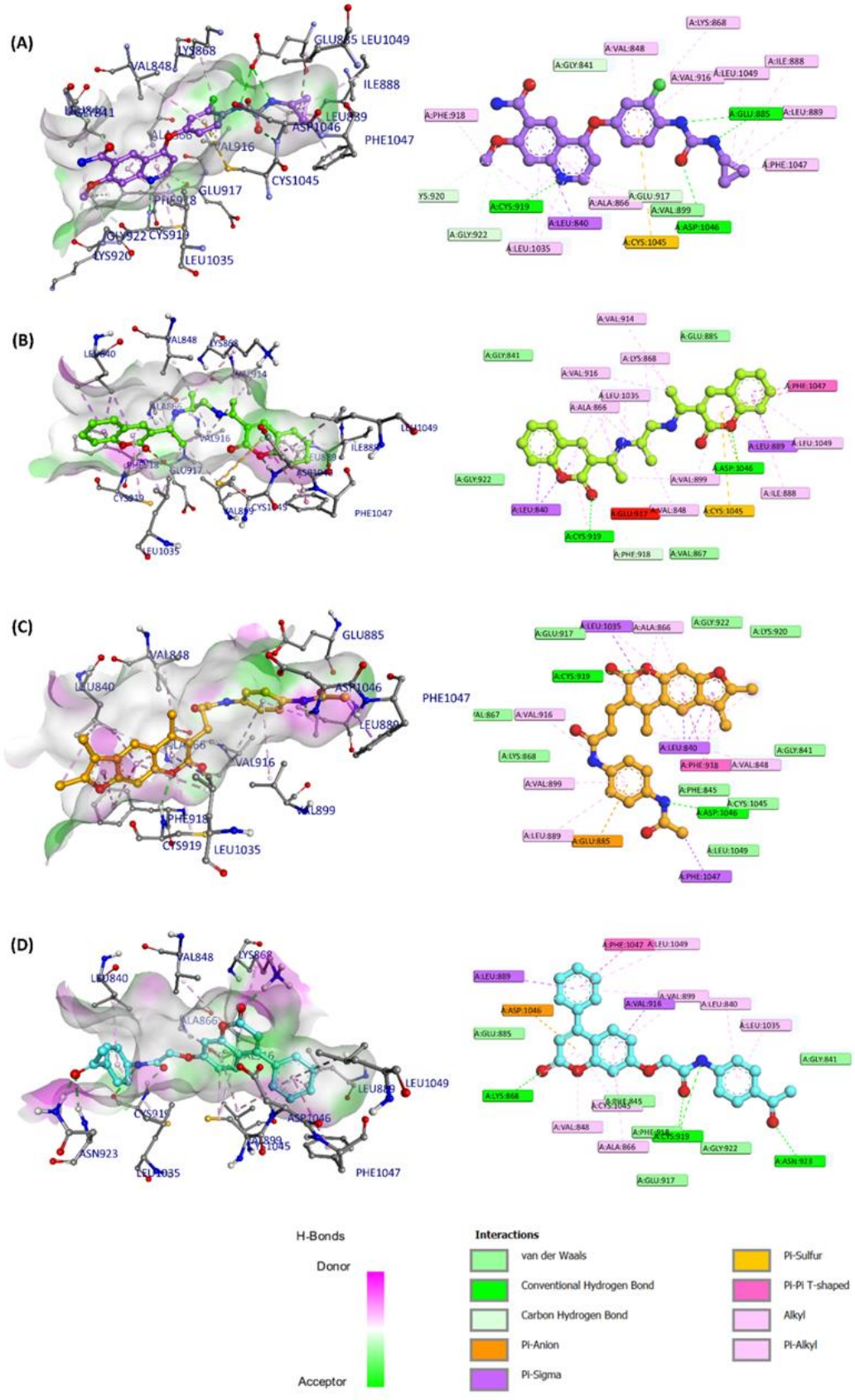

Figure 3.5 3D and 2D interaction diagram of best hits obtained via HTVS with VEGFR-2 protein (PDB Id. 3WZD). (A) Lenvatinib, (B) CNP0056360, (C) CNP0340213, and (D) CNP0366287.

3.3.6 *In silico* ADMET prediction

The *in silico* ADMET profiling gives primitive information about the pharmacokinetics of virtually identified leads. The different parameters viz. Blood-brain barrier (BBB) permeation, Aqueous solubility, Human Intestinal Absorption (HIA), hERG inhibition, rodent carcinogenicity, plasma protein binding (PPB), CYP2D6 inhibition, and Rule of Five (Ro5) violation are important in deciding if the molecule will be successful in drug discovery pipeline. The BBB penetration is a crucial parameter as the CNS active drugs are required to penetrate BBB while CNS inactive drugs should not cross BBB. The classification used by PreADMET for BBB penetration is BB (C_{brain}/C_{blood}) > 2.0- High CNS absorption, between 2.0 to 0.1- Moderate CNS absorption, and < 0.1- Low CNS absorption [121]. The PPB controls the amount of drug available in plasma for pharmacological action. According to PreADMET, PPB% > 90% is strong binding, while PPB% < 90% is weak binding. The aqueous solubility of a drug is essential for its absorption and subsequent action. HIA represents the absorption of orally administered drugs from the gastrointestinal system into the bloodstream. The %HIA between 0-20, 20-70, and 70-100 indicates poor, moderate, and high absorption, respectively. The hERG inhibition results in cardiotoxicity by prolongation of the QT interval. Hence, it is important to determine if a lead has high or medium risk for hERG inhibition. CYP2D6 enzymes are responsible for the metabolism of approximately 20% of drugs, and thus, their inhibition will reduce drug metabolism and increase toxicity. Rodent carcinogenicity is determined to extrapolate its carcinogenic effects in humans. The Rule of Five (Ro5) is considered important to predict the drug-likeness of a molecule. The general paradigm is- for a molecule to become drug-like, it must fall within the permissible limits of Ro5 but, in many NPs inspired FDA approved drugs this is not true. The ADMET profile of compounds CNP0056360, CNP0340213, and CNP036628 was comparatively better than

rest of the compounds as shown in Table 3.2. The *in silico* ADMET properties of rest of the compounds is provided in Appendix (Table A.2).

Table 3.2 ADMET prediction of final hits.

	CNP0056360	**CNP0340213**	**CNP0366287**
BBB	0.625	0.049	0.019
Water Solubility	Moderately Soluble	Moderately Soluble	Moderately Soluble
HIA (%)	98.18	95.02	96.45
hERG Inhibition	Medium Risk	Medium Risk	Medium Risk
PPB (%)	88.46	89.91	96.23
Rodent Carcinogenicity	Non-Carcinogen	Non-Carcinogen	Non-Carcinogen
CYP2D6 Inhibitor	Non-Inhibitor	Non-Inhibitor	Non-Inhibitor
Lipinski's Ro5 Violations	Zero	Zero	Zero

3.3.7 MD simulation study

To check the binding of CNP0056360, CNP0340213, and CNP036628 with VEGFR-2 in a real-time simulated environment and study the ligand-protein interaction in detail, the MD studies were performed. The RMSD is the measure of average deviation in the position or coordinates of an atom in a particular frame compared to the reference frame [122]. Typically, the perfect overlap of structure is inevitable, so it is desirable to obtain minimum deviation to ensure protein stability. The protein's structural conformation can be understood by monitoring its RMSD throughout the MD simulation. The average RMSD of protein between 1-3 Å is considered acceptable for small globular proteins. The ligand RMSD gives insights into the ligand-protein interactions as it enables assessment of stability about protein and its binding pocket. When the ligand RMSD values significantly exceed that of protein, it indicates that the ligand may have moved away from the binding pocket.

The average RMSD for VEGFR-2 complexed with CNP0056360, CNP0340213, CNP036628, and lenvatinib was found to be 1.0161, 1.7137, 1.6695, and 1.5233 Å, respectively. CNP0056360-VEGFR-2 complex exhibited the lowest RMSD, even smaller

than lenvatinib indicating better protein. The RMSD of VEGFR-2 bound to the two ligands were slightly higher than the lenvatinib-VEGFR-2 complex. The mean ligand RMSD for CNP0056360, CNP0340213, CNP036628, and lenvatinib when bound to VEGFR-2 was found to be 1.4949, 0.9353, 1.6727, and 0.8356 Å, respectively. There was not much variation between ligand and protein RMSD of three ligands and lenvatinib, indicating that ligands didn't diffuse out of binding pocket during simulation run (Figure 3.6).

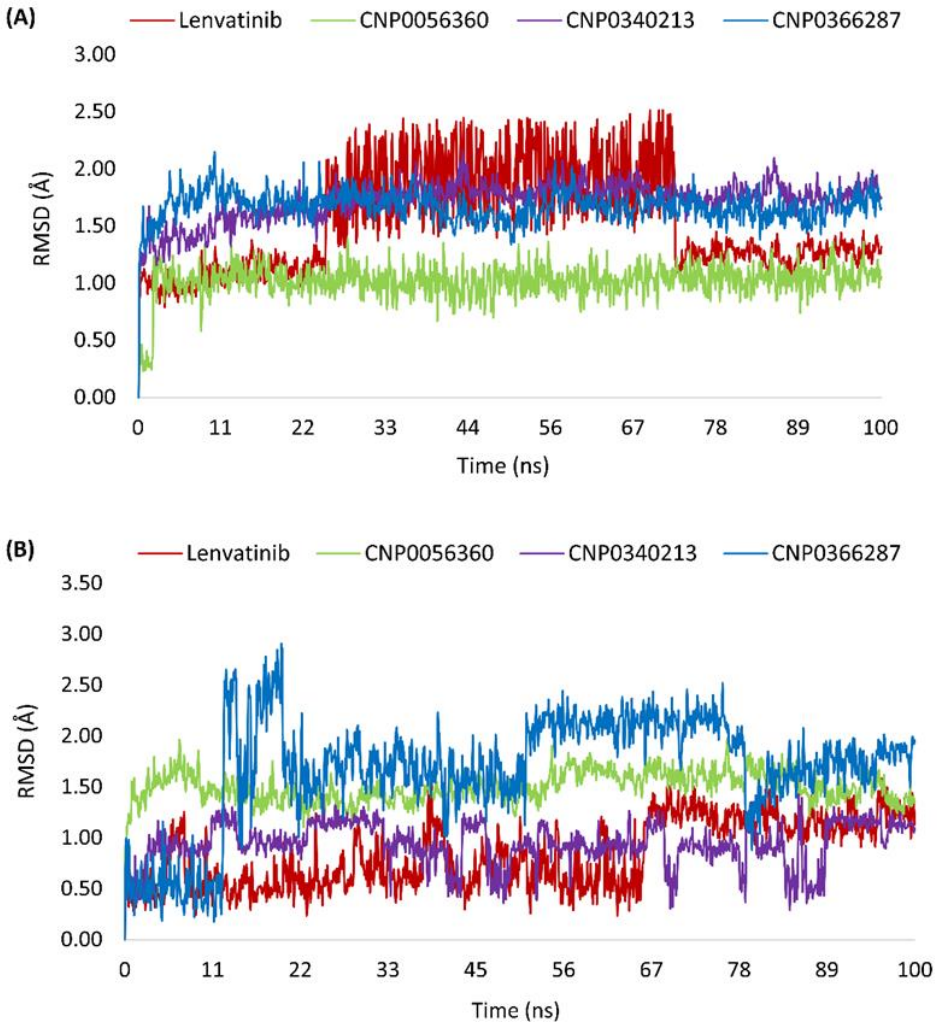

Figure 3.6 RMSD plot of complexes with VEGFR-2 protein. (A) RMSD of the protein-ligand complexes (Lenvatinib (red), CNP0056360 (green), CNP0340213 (purple), CNP0366287 (blue)). (B) RMSD of heavy atoms of the ligands (Lenvatinib (red), CNP0056360 (green), CNP0340213 (purple), CNP0366287 (blue)).

The RMSF monitoring gives an idea about the flexibility and local changes occurring in the protein during the simulation run. In general, a high fluctuation is observed in the C- and N-terminal compared to other parts. In the RMSF plot, peaks specify protein residues that fluctuate most. The average RMSF values for VEGFR-2 complexed with CNP0056360, CNP0340213, CNP036628, and lenvatinib were 1.105, 1.1258, 1.1194, and 1.128 Å, respectively. The high fluctuations were observed in the tail region which are inevitable. The high fluctuations near residues 840-890, 915-925, and 1035-1050 could be seen in Figure 3.7 because they are active site residues and involved in interacting with the ligands. The residues Cys919 and Asp1046 are involved in H-bond interaction, showing high fluctuations in the RMSF plot. Other than active site residues, the rest of the protein was stable throughout the run.

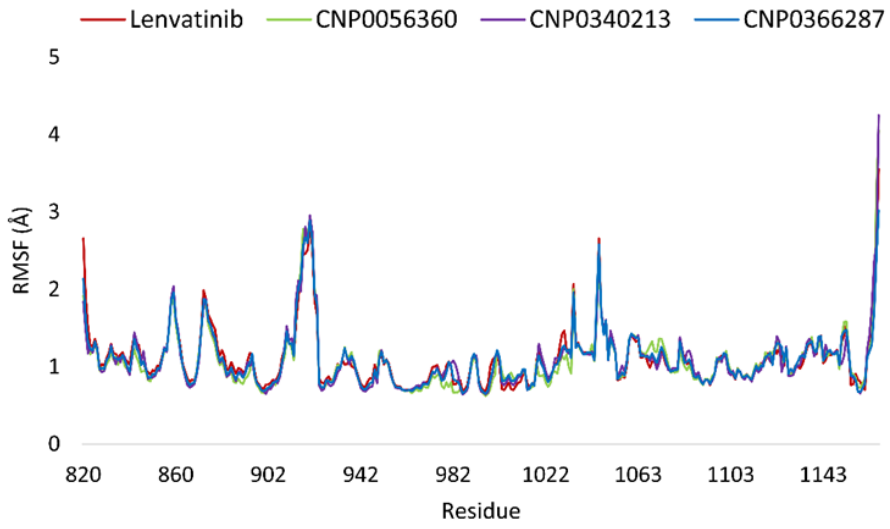

Figure 3.7 Residue-wise RMSF deviation of complexes (Lenvatinib (red), CNP0056360 (green), CNP0340213 (purple), CNP0366287 (blue)).

Hydrogen bonds are crucially involved in the binding of ligands with the protein's active site. The H-bond analysis is important as it highly influences absorption and metabolism of drugs. The H-bond is also essential for stabilizing the protein-ligand complex and is indicative of strong and stable binding. Lenvatinib showed maximum two H-bond interactions present at most of the simulation time. In case of CNP0056360, the maximum

number of H-bond interactions observed was four that kept varying between two and three, and one H-bond was present at most of the run. Except for CNP0056360, no ligand including lenvatinib showed four H-bond interactions. For CNP0340213, three H-bond interactions were observed at the start of simulation that reduced to two and subsequently one. In CNP0366287, one H-bond interaction was present for almost whole run while two and three H-bonds were present only for a brief period of time (Figure 3.8).

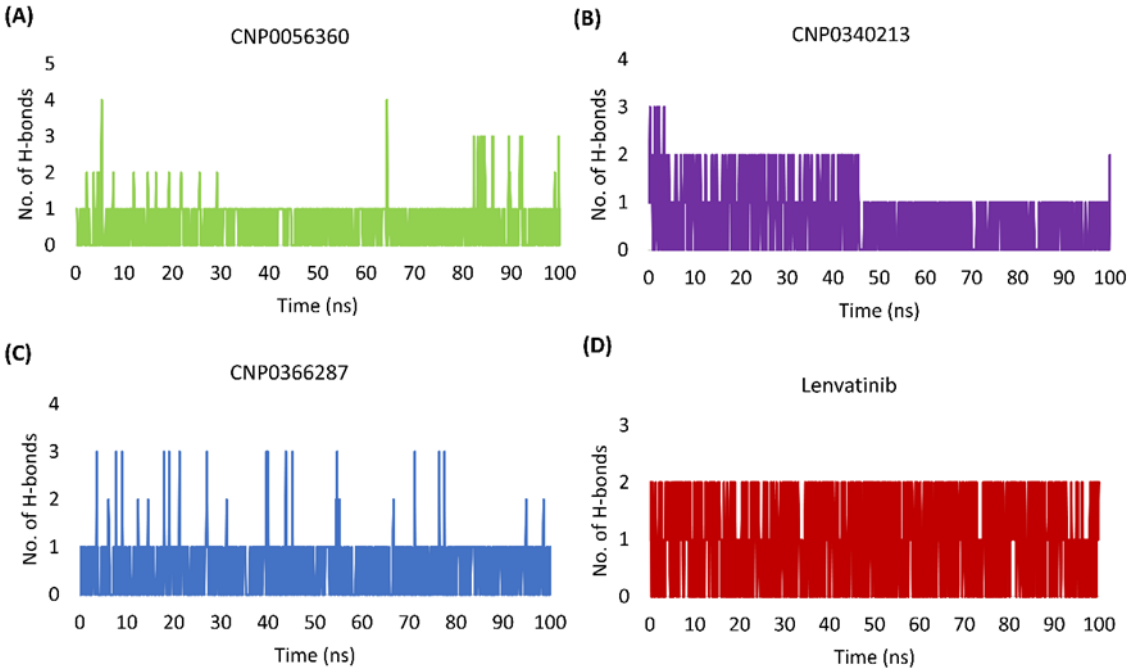

Figure 3.8 Number of intermolecular H-bond interactions shown by the ligand during simulation run (A) CNP0056360, (B) CNP0340213, (C) CNP0366287, and (D) Lenvatinib.

Rg calculated to get information regarding conformational change in protein structure [46]. The average Rg values for CNP0056360-VEGFR-2 complex, CNP0340213-VEGFR-2 complex, CNP0366287-VEGFR-2 complex, and Lenvatinib-VEGFR-2 complex were 20.2873 Å, 20.3322 Å, 20.3348 Å, and 20.4940 Å, respectively (Figure 3.9).

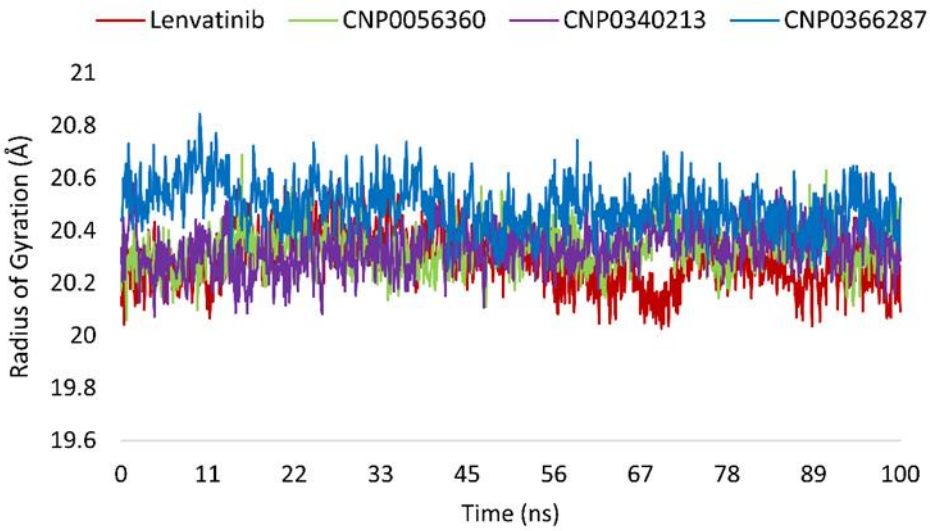

Figure 3.9 The radius of gyration of complexes (Lenvatinib (red), CNP0056360 (green), CNP0340213 (purple), CNP0366287 (blue)).

3.3.8 Binding free energy calculation

The prediction of binding energy between ligand and protein is achieved through free energy calculations. These methods analyze the atomic-level interactions that contribute to the ligand affinity for protein [122]. Within the framework of MM-GBSA and MM-PBSA calculations, the calculation involves the assessment of both molecular mechanics (MM) and solvation energies. The solvation energy encompasses two components: a polar component (evaluated using an implicit solvent model (PB or GB)) and a non-polar component [110].

Table 3.3 and Table 3.4 display the non-bonded interaction energies (van der Waals energy- ΔE_{vdw}, electrostatic energy- ΔE_{ele}, polar part of solvation free energy- ΔG_{PB}, nonpolar part of solvation free energy- $\Delta G_{Nonpolar}$, and total binding free energy- ΔG_{MMPBSA}) for all the complexes analyzed using the MM-GBSA and MM-PBSA methods, respectively. Both approaches demonstrated low overall binding energies, indicating a high level of stability in the complexes. The gas phase energies, specifically ΔE_{vdw} and ΔE_{ele}, substantially contribute to the overall stability, suggesting that confirming the ligand relative to the receptor is the primary factor in complex stability.

Among the identified compounds, CNP0056360 and CNP0340213 exhibited stronger binding free energy than lenvatinib in the GB model. In the PB model, CNP0056360 and CNP0340213 exhibited stronger binding free energy than lenvatinib.

Table 3.3 Energy contributions of complexes obtained from MM-GBSA.

Energy Component	CNP0056360	CNP0340213	CNP0366287	Lenvatinib
$\Delta E_{vdw(kcal/mol)}$	-72.3401 ± 1.3761	-65.2911 ± 1.2701	-66.1271 ± 2.2427	-59.7153 ± 1.3934
$\Delta E_{ele(kcal/mol)}$	-4.3141 ± 0.6579	-11.1043 ± 1.4064	3.466 ± 6.2043	8.2341 ± 3.4526
$\Delta G_{GB(kcal/mol)}$	21.791 ± 0.4934	26.1831 ± 1.3598	27.5681 ± 6.7112	12.9643 ± 2.8223
$\Delta G_{SA(kcal/mol)}$	-7.3457 ± 0.0401	-6.9151 ± 0.106	-7.6897 ± 0.1063	-6.759 ± 0.0596
$\Delta G_{MMGBSA(kcal/mol)}$	-62.209 ± 1.6631	-57.1274 ± 1.3944	-42.7827 ± 1.9897	-45.2759 ± 1.3402

Data expressed in Mean ± SEM (*n*=5)

Table 3.4 Energy contributions of complexes obtained from MM-PBSA.

Energy Component	CNP0056360	CNP0340213	CNP0366287	Lenvatinib
$\Delta E_{vdw(kcal/mol)}$	-72.3401 ± 1.3761	-65.2911 ± 1.2701	-66.1271 ± 2.2427	-59.7153 ± 1.3934
$\Delta E_{ele(kcal/mol)}$	-4.3141 ± 0.6579	-11.1043 ± 1.4064	3.466 ± 6.2043	8.2341 ± 3.4526
$\Delta G_{PB(kcal/mol)}$	25.7312 ± 1.118	31.5521 ± 1.3665	26.3881 ± 6.808	9.4164 ± 4.6718
$\Delta G_{Non-Polar(kcal/mol)}$	-4.2468 ± 0.0228	-4.3451 ± 0.0979	-4.6465 ± 0.0187	-4.5083 ± 0.0354
$\Delta G_{MMPBSA(kcal/mol)}$	-55.1698 ± 2.3583	-49.1885 ± 2.0212	-40.9194 ± 1.966	-46.5731 ± 2.0084

Data expressed in Mean ± SEM (*n*=5)

3.4 Conclusion

In this study, the COCONUT database was investigated through rigorous pharmacophore-based virtual screening approach to identify coumarin leads as VEFR-2 inhibitors, a crucial target in cancer treatment. The study employed multi-stage virtual screenings using lenvatinib as a standard for comparison. The study revealed three hits-CNP0056360, CNP0340213, and CNP0366287 with favorable binding energies and acceptable *in silico* ADMET properties. MD simulations of all three hits in a simulated biological environment demonstrated favorable stability when bound to the VEGFR-2. CNP0056360 formed the most stable complex with extensive and consistent H-bond interactions with VEGFR-2. The binding free energy calculations also revealed the superior binding free energies of CNP0056360 and CNP0340213 compared to lenvatinib

in both solvation models. Overall, these leads displayed favorable binding profiles, good stability in complex with VEGFR-2, and potentially superior binding affinities compared to lenvatinib. The study findings demonstrated effectiveness and potential of identified leads as inhibitors of VEGFR-2. While further *in vitro* and *in vivo* studies are necessary to validate these findings, the current results establish a strong foundation for developing novel coumarin-based VEGFR-2 inhibitors for cancer therapy. With successful experimental validation and continued research, these leads have the potential to translate into novel and effective cancer treatment options.